

Revealing behavioral impact on mobility prediction networks through causal interventions

Ye Hong^{a,*}, Yanan Xin^a, Simon Dirmeier^b, Fernando Perez-Cruz^{b,c}, Martin Raubal^a

^a*Institute of Cartography and Geoinformation, ETH Zurich*

^b*Swiss Data Science Center, ETH Zurich and EPFL*

^c*Institute for Machine Learning, Department of Computer Science, ETH Zurich*

Abstract

Deep neural networks are increasingly utilized in mobility prediction tasks, yet their intricate internal workings pose challenges for interpretability, especially in comprehending how various aspects of mobility behavior affect predictions. This study introduces a causal intervention framework to assess the impact of mobility-related factors on neural networks designed for next location prediction – a task focusing on predicting the immediate next location of an individual. To achieve this, we employ individual mobility models to generate synthetic location visit sequences and control behavior dynamics by intervening in their data generation process. We evaluate the interventional location sequences using mobility metrics and input them into well-trained networks to analyze performance variations. The results demonstrate the effectiveness in producing location sequences with distinct mobility behaviors, thereby facilitating the simulation of diverse yet realistic spatial and temporal changes. These changes result in performance fluctuations in next location prediction networks, revealing impacts of critical mobility behavior factors, including sequential patterns in location transitions, proclivity for exploring new locations, and preferences in location choices at population and individual levels. The gained insights hold significant value for the real-world application of mobility prediction networks, and the framework is expected to promote the use of causal inference for enhancing the interpretability and robustness of neural networks in mobility applications.

Keywords: Mobility behavior, Domain shift, Individual mobility simulation, Next location prediction, Causal intervention.

*Corresponding author

Email addresses: hongy@ethz.ch (Ye Hong), yanxin@ethz.ch (Yanan Xin), simon.dirmeier@sdsc.ethz.ch (Simon Dirmeier), fernando.perezacruz@sdsc.ethz.ch (Fernando Perez-Cruz), mraubal@ethz.ch (Martin Raubal)

1. Introduction

Accurate individual mobility prediction plays a pivotal role in popularizing emerging mobility services (Ma and Zhang, 2022) and serves as a crucial backbone for various intelligent transport systems functionalities (Tang et al., 2019). Proactively offering predictions of individual mobility profoundly influences customer satisfaction and system efficiency (Zhao et al., 2018), making it indispensable for successfully decarbonizing the transport sector (Hong et al., 2022). Despite its considerable application potential, individual mobility prediction remains a challenging problem due to the complex mobility patterns, influenced by a wide range of behavioral factors and mobility-related contexts (Hong et al., 2023b). The intricacies in modeling these spatiotemporal dependencies generally hinder achieving perfect predictions of individual mobility (Song et al., 2010b; Barbosa et al., 2018; Wiedemann et al., 2023a). In recent years, the availability of human digital traces and the advancements in data-driven models, particularly deep neural networks capable of capturing spatiotemporal dynamics, have significantly enhanced mobility prediction ability (Luca et al., 2021).

Although modern neural networks have achieved solid predictive performance, they have often faced criticism for their low interpretability (Manibardo et al., 2022; Pappalardo et al., 2023), referring to the degree to which humans can comprehend the decision-making process of a model. These networks are commonly regarded as “black boxes” because it is challenging to reconstruct the reasoning that leads to a particular prediction. In the context of mobility prediction, the lack of interpretability translates to an unclear understanding of which spatiotemporal patterns the network has captured and, more fundamentally, the roles played by various behavioral factors in making predictions. As a result, this deficiency negatively impacts decision-making and policy design, and also affects perceived reliability and trustworthiness by the practitioners (Huang et al., 2020), thus impeding the seamless integration of mobility prediction networks into real-world application systems (Koushik et al., 2020). Furthermore, the scarcity of publicly available individual mobility data sets, primarily due to the privacy-sensitive nature of personal mobility (Wiedemann et al., 2023b), leads to a lack of comparability between existing and newly developed mobility prediction models (Graser et al., 2023), further exacerbating the interpretability issue. Consequently, prediction networks are evaluated using data sets featuring varying numbers and types of participants, along with differing tracking durations, representing diverse snapshots of the possible mobility behavior (Kulkarni and Garbinato, 2019). Hence, a comprehensive analysis revealing the impact of behavior dynamics on prediction performance is imperative to establish data specifications that can serve as benchmarks for evaluating neural networks employed in mobility studies.

In addition, establishing connections between mobility behaviors and prediction performances reveals the robustness of these networks when confronted with unforeseen inputs. The neural network optimization requires a training data set, leading to the widely acknowledged fact that their performances depend on the quality and representativeness of the training data (Yin et al., 2022). However, individual mobility behavior constantly changes over space and time (Xu et al., 2018a; Hong et al., 2023a). The mobility data encountered by the prediction network during application often reflects a distinct mobility behavior compared to the data on which the network was trained. This leads to a discrepancy between the training and testing data distributions, a phenomenon known as domain shift (He et al., 2020; Xin et al., 2022). Enhancing our understanding of the performance under various shift scenarios is essential to assess the reliability when applying these networks across diverse geographic regions or time periods. Yet, this relationship remains predominantly unexplored.

Causal intervention offers a promising tool for generating data from diverse environments, enabling the assessment of neural network robustness and providing human-friendly causal explanations for these interventions (Xin et al., 2022). Building upon the advantages of this approach, we present a framework for systematically evaluating the impact of mobility behaviors on the performance of prediction networks. Specifically, this framework utilizes individual mobility models capable of simulating mobility traces, and employs causal intervention strategies in the data generation process, allowing for flexible modifications of the defined mobility behavior. We subsequently assess the performance of trained neural networks on these synthetic traces for mobility prediction. Our study focuses on next location prediction – a mobility prediction task aiming to forecast the immediate next location of an individual based on their mobility history. The conducted interventions simulate realistic spatial and temporal changes in mobility patterns, leading to performance fluctuations in prediction networks that reflect their robustness when confronted with domain shifts. This framework facilitates assessing the impact of behavioral factors and benchmarking mobility prediction networks, with practical applications for evaluating network performances and transferring these networks across domains. In short, our contributions are summarized as follows:

- We introduce a framework to assess the robustness of mobility prediction networks through causal intervention. This framework enables direct control over behavioral dynamics, quantifying ensuing mobility patterns, and evaluating their influence on network performance.
- We employ this framework to simulate diverse spatiotemporal shift scenarios, thereby improving the interpretability of prediction networks, and demonstrating its efficacy in benchmarking mobility data sets and identifying performance degradation during real-world applications.

- We open-source the framework, enabling straightforward utilization and flexible customization of its components¹.

The rest of this paper is organized as follows: Section 2 offers a systematic review of related work. We then introduce details of the robustness assessment framework in Section 3. Section 4 provides information about the empirical movement dataset and experimental design choices. Section 5 reports results obtained by applying the framework across various scenarios, followed by a discussion in Section 6. Finally, we summarize key findings and conclude the paper in Section 7.

2. Related work

2.1. Mobility behavior and its impact on mobility prediction

Research on individual mobility behavior, with a strong emphasis on spatiotemporal patterns of activities and trips, has consistently been at the forefront of mobility studies (Chen et al., 2016), propelling theoretical and methodological advancements within the activity-based analysis framework (Schönfelder and Axhausen, 2016). In this framework, trips are perceived as an induced demand resulting from the necessity to engage in activities at distinct spatial locations (Axhausen and Gärling, 1992), making the selection of activity locations a pivotal aspect in comprehending individual mobility behavior (Hong et al., 2023a). Over the years, studies have consistently shown that location choices not only vary across populations (inter-person variability) (Martin et al., 2023b; Ji et al., 2023) but also undergo constant changes over time (intra-person variability) (Susilo and Axhausen, 2014; Hintermann et al., 2023). Furthermore, decisions regarding activity locations are frequently influenced by various external factors, some of which, when encountered, can lead to sudden structural changes, such as residential relocation (Ramezani et al., 2021) and large-scale crises (Santana et al., 2023). These empirical insights emphasize the need to study activity location choices from a dynamic perspective, rather than approaching them solely with static mobility snapshots.

Considering the central role of activity in shaping individual mobility, activity location prediction serves as a crucial component in mobility ahead planning and optimization (Sun and Kim, 2021; Ma and Zhang, 2022). Within this context, predicting the immediate next location of an individual has garnered widespread attention (Luca et al., 2021). Accurately inferring the next location is influenced not only by the capability of the employed predictive network but also by the behavioral patterns of individuals. In a pioneering

¹The source code is available at <https://github.com/irmlma>

effort to link mobility behavior with location prediction, [Song et al. \(2010b\)](#) proposed entropy as a measure for the theoretical mobility predictability based on visited location sequences of individuals. Their study revealed remarkably consistent predictability across individuals, peaking at approximately 93% in the tested dataset, reflecting inherent travel patterns across various demographic attributes ([Song et al., 2010b](#)). Although studies have highlighted their strong correlation with actual prediction performance ([Lu et al., 2013](#)), entropy-related predictability measures remain challenging to interpret ([Teixeira et al., 2019](#)). Consequently, recent research has started to represent mobility behavior with more straightforward metrics, such as routine and novelty components ([Teixeira et al., 2021](#)), usages of transport services ([Xu et al., 2022](#)) and recurring patterns in daily mobility ([Hong et al., 2023b](#)), and analyze its impact on prediction performance. Nevertheless, our comprehension of their connections is still in its early stages, relying on insights derived from observed mobility behavior within available movement tracking data sets, which often exhibit limited behavior variability and biased behavior distribution.

2.2. Causal intervention and its application in robustness assessment

The field of causal modeling, dedicated to investigating causal relationships, provides a systematic framework for managing the generation of mobility traces that depict specific mobility behaviors. Causal modeling necessitates establishing a structural causal model (SCM) to clarify the factors and their interconnections in a data generation process ([Rahimi et al., 2023](#)). With access to a particular SCM, we can perform causal interventions on individual factors or combinations thereof, effectively disentangling intricate interactions among causal variables by unilaterally adjusting the value of a single variable and observing its impact on the generated data ([Pearl and Mackenzie, 2018](#)). These strategies have already found practical applications across diverse domains. For instance, in prognostic research, causal intervention has been applied to forecast risks associated with various medical treatments ([van Amsterdam et al., 2019](#)), examine the impact of therapy on the cognitive development of prematurely born infants ([Silva, 2016](#)), and investigate the effects of demographic variations on brain structure using counterfactual samples ([Pawlowski et al., 2020](#)). Similar methods have also been applied in climate and earth science to unravel the complexities of spatiotemporal dynamic processes ([Li et al., 2023](#); [Runge et al., 2023](#)).

In particular, causal intervention methods have shown the potential to evaluate and enhance the robustness of machine learning models across various domains ([Schölkopf et al., 2021](#)). A common technique involves data augmentation through interventions on non-causal style features that do not affect the predicted label ([Mao et al., 2021](#); [Moshkov et al., 2024](#)). Similarly, in mobility analysis, causal interventions facilitate data generation from either in-distribution or out-of-distribution (OoD) by selecting variables sub-

ject to intervention and adjusting the intervention strength using mechanistic mobility simulators. Over the past decade, these simulators have significantly advanced in replicating high-level spatiotemporal properties of individual movements (Pappalardo et al., 2023), and have seen increasing application in generating synthetic individual mobility traces for large-scale simulations (Xu et al., 2018b; Barbosa et al., 2018). Notable examples include the exploration and preferential return (EPR) model (Song et al., 2010a), the location attractiveness model (Yan et al., 2017), and the container model (Alessandretti et al., 2020), all of which introduce parameters to replicate certain aspects of mobility behavior. These simulators feature inherent causal structures that facilitate their transformation into SCMs and can be effectively leveraged within a causal intervention framework. In this study, performing causal interventions for mobility models enables us to generate a wide spectrum of mobility behaviors that adhere to realistic behavior distributions, facilitating the robustness assessment of prediction networks when confronted with domain shifts.

3. Methodology

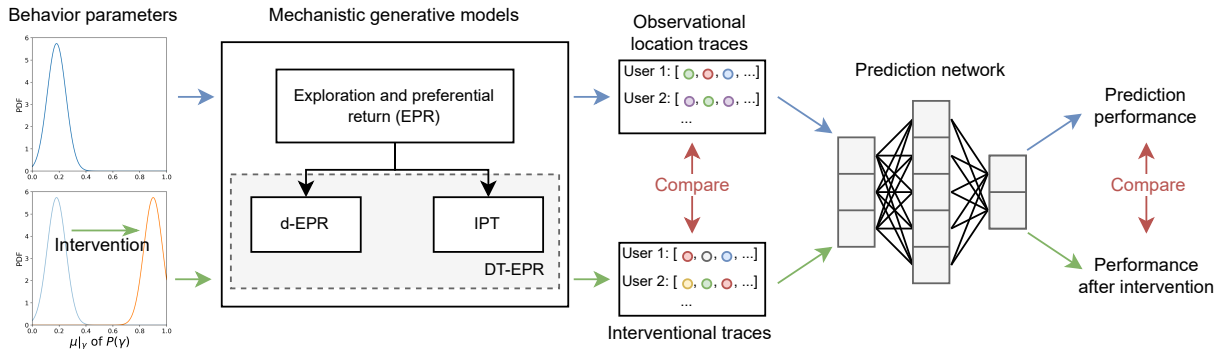


Figure 1: Evaluating the robustness of prediction networks through causal interventions. Synthetic location sequences are obtained from mechanistic generative models and fed into location prediction networks to evaluate performance (blue arrows). This process is repeated for interventional location sequences, obtained by modifying the empirical distributions (green arrows). The differences in mobility patterns and prediction performances are compared to assess intervention strengths and network robustness (red arrows).

The overall pipeline for assessing the robustness of prediction networks is illustrated in Figure 1. We start by introducing mechanistic generative models for synthesizing individual location sequences (§3.1). These models incorporate parameters to replicate real-world observational mobility behavior. Subsequently, we perform interventions by modifying the parameters, thereby manipulating mobility behaviors and allowing us to generate new interventional location sequences (§3.2). Lastly, we employ networks trained for next location prediction to process both the observational and interventional location sequences (§3.3). We quantify the change in prediction performance to evaluate the robustness of prediction networks. In this study, the term

location refers specifically to a geographical place where individuals engage in activities (Martin et al., 2023a). This excludes other types of points, such as waypoints on roads (e.g., GPS recordings) or intermediate stops without any meaningful activity (e.g., waiting for a bus). We provide a more detailed description of each module in the following sections.

3.1. Individual mobility models

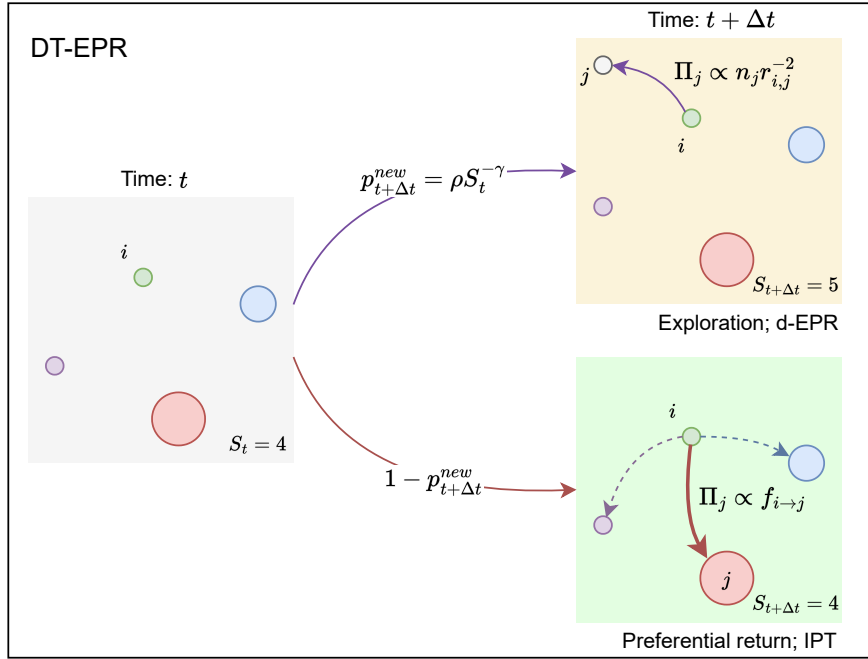


Figure 2: Illustration of the mechanistic generative model density transition (DT)-EPR. The individual at location i visited $S_t = 4$ locations with a frequency proportional to the size of the location circle at time t . At time $t + \Delta t$, the individual chooses to either explore a new location with probability $p_{t+\Delta t}^{new}$, where the next location j will be chosen based on its population attractiveness n_j and the travel distance $r_{i,j}$ (density (d)-EPR mechanism; upper panel), or return to a previously visited location with complementary probability $1 - p_{t+\Delta t}^{new}$, where the location probability Π_j is proportional to the empirical visit frequency from i (individual preferential transition (IPT) mechanism; lower panel). Thus, DT-EPR combines the location exploration mechanism from d-EPR and the preferential return mechanism from IPT. Figure adapted from Song et al. (2010a).

Individual mobility models aim to simulate realistic movement trajectories based on a predefined set of behavioral parameters, allowing for direct control over the mobility behavior of the generated population. We start with the EPR model (Song et al., 2010a) as our baseline SCM and additionally introduce two EPR-based generative models, namely density (d)-EPR (Pappalardo et al., 2015) and individual preferential transition (IPT) (Zhao et al., 2021). We finally propose the density transition (DT)-EPR model that combines the advantages of d-EPR and IPT to obtain more realistic mobility traces. Figure 2 delineates the mechanisms of DT-EPR and its connection with d-EPR and IPT models.

EPR generates sequences of location visits for individuals and reproduces observed scaling laws for dis-

tinct location numbers and their visitation frequency over time (González et al., 2008; Barbosa et al., 2018), both of which are important properties affecting the performance of next location prediction networks (Hong et al., 2022). The core of EPR is the introduction of two competing mechanisms, exploration and preferential return, into traditional random-walk models (Brockmann et al., 2006). These two mechanisms account for the tendency of individuals to return to previously visited locations (Song et al., 2010a). Specifically, observing an individual at location i at time t , the model assumes that the individual will change their location after a waiting time Δt , where Δt is sampled from its distribution $P(\Delta t)$. The individual chooses to explore a previously unvisited location with probability $p_{t+\Delta t}^{new}$:

$$p_{t+\Delta t}^{new} = \rho S_t^{-\gamma} \quad (1)$$

where $0 < \rho \leq 1$ and $\gamma \geq 0$ are parameters that control the exploration tendency and S_t denotes the number of distinct location visited until time t . During this process, a new location is determined by sampling a moving distance Δr from the jump length distribution $P(\Delta r)$, with the moving direction chosen uniformly at random. After the move, the number of visited locations increases from S_t to $S_t + 1$. Besides exploring a new location, the individual could return to a visited location with complementary probability $1 - p_{t+\Delta t}^{new}$. In this case, the probability of moving to a location j , denoted as Π_j , is proportional to the number of previous visits to j , i.e., $\Pi_j \propto f_j$, where f_j is the visitation frequency of j .

Later variants of EPR have modified the search for locations in order to replicate spatial patterns. One such variant is the d-EPR model, which addresses the insufficient reproduction of the evolution of the radius of gyration (Pappalardo et al., 2015). A population attractiveness factor is assigned to each location to model the tendency to visit popular locations (Figure 2 upper panel). In the model, the probability Π_j of selecting location j during exploration depends on its travel distance and attractiveness:

$$\Pi_j \propto n_j r_{i,j}^{-2} \quad (2)$$

where $r_{i,j}$ is the distance between the current location i and the new location j , and n_j denotes the attractiveness, quantified as the empirical visits by all individuals to location j . Furthermore, a subsequent study has identified that individuals can travel arbitrarily large distances during preferential return, as the location selection of EPR is based solely on empirical visit frequency (Zhao et al., 2021). To address this limitation, Zhao et al. (2021) proposed the IPT model that constrains the preferential return to be conditioned on the current location, i.e., imposing a first-order Markov process on location choices (Figure 2 lower panel). The

visit probability of location j is defined as proportional to the number of previous visits from the current location i to j :

$$\Pi_j \propto f_{i \rightarrow j} \quad (3)$$

In practice, a personalized Markov transition matrix containing $f_{i \rightarrow j}$ for each location pair is initialized from empirical location visits and updated during the generation process.

We combine the exploration mechanism of d-EPR and the preferential return mechanism of IPT to introduce a new EPR-based model, which we refer to as DT-EPR (Figure 2). Consequently, DT-EPR inherits the capacity to capture both population attractiveness and individual preferences in location choices, and is expected to replicate realistic location visit sequences.

As a result, for each individual u^i in the user set $\mathcal{U} = \{u^1, \dots, u^{|\mathcal{U}|}\}$, DT-EPR generates a time-ordered trajectory $T^i = (L_k)_{k=1}^{m_{u^i}}$ composed of m_{u^i} locations visited by u^i . A location L contains spatiotemporal information and is represented as a tuple of $L = \langle l, p, t \rangle$, where l is the location identifier, $p = \langle x, y \rangle$ represents spatial coordinates in a reference system, e.g., latitude and longitude, and t is the time of visit. Thus, we construct the location set \mathcal{O}^i containing the known location identifiers for individual u^i , and the set $\mathcal{O} = \{\mathcal{O}^1, \dots, \mathcal{O}^{|\mathcal{U}|}\}$ including all locations in the data set.

3.2. Intervention design

The DT-EPR model can be used as a generative, mechanistic simulator to obtain mobility sequences. Specifically, we empirically estimate the parameter distributions from a tracking data set and use these distributions to simulate data from the model, generating synthetic *observational* mobility traces. Since DT-EPR is a parametric simulator, i.e., parameters have real-world interpretations with explainable, statistical relationships with the other model variables, we can introduce causal interventions to data-generating processes to simulate *interventional* mobility trajectories. Causal interventions can be interpreted as shifts in the observed mobility patterns, representing various scenarios, such as spatial shifts when certain locations become more or less attractive or temporal shifts in mobility behavior between seasons or years.

Considering the modeling mechanisms of the DT-EPR model, we perform interventions on the following parameters to simulate comprehensive behavior shift scenarios:

- The exploration tendency p^{new} , affecting whether or not to explore in the next time step (Eq. 1). While the number of distinct locations collectively exhibits sublinear growth (Song et al., 2010a), notable inter-person variability in location choices implies substantial variations in the exact exploration speed among individuals (Hong et al., 2023a). In EPR-like models, p^{new} is determined by parameters ρ and

γ , independently sampled for each individual from empirical distributions. We introduce interventions on ρ and γ by altering their empirical distributions, producing pseudo-populations with different exploration behaviors. Formally, let $\mathbb{P}_{\mathcal{S}}^{(\rho, \gamma, p^{new})}$ be the joint probability distribution over random variables ρ, γ, p^{new} induced by the SCM \mathcal{S} . We intervene on each these variables, e.g., for the case of ρ we set $\mathbb{P}_{\mathcal{S}}^{(\rho, \gamma, p^{new})|do(\rho=\tilde{f}_{\rho}(\cdot))}$, meaning we replace the generating mechanism of ρ with a new one \tilde{f}_{ρ} . The intervention $do(\rho = \tilde{f}_{\rho}(\cdot))$ induces a new probability distribution $\mathbb{P}_{\mathcal{S}}^{(\rho, \gamma, p^{new})}$ with modified structural equations that we use for sampling interventional data. Additionally, we perform hard interventions on p^{new} by fixing its value to a constant. This intervention removes the time-dependent modeling of location exploration, falling back to the assumption in the Lévy flight model (Brockmann et al., 2006). Employing the same formalism as above, a hard intervention puts point mass on a specific outcome of a structural equation, such that we denote the intervention as $do(p^{new} = a)$, where a is a constant value.

- The population attractiveness n , affecting location choices during exploration (Eq. 2). We manipulate location attractiveness to simulate changes in the spatial preferences of the population. To retain location visitation characteristics, we randomly shuffle empirical visit numbers for a group of locations to create synthetic mobility traces. The strength of the intervention can then be controlled by adjusting the group of locations, e.g., including more locations in the shuffling process introduces a more substantial intervention.
- The empirical individual preference f , affecting location choices during preferential return (Eq. 3). As individual mobility behavior is dynamic and varies considerably over time, we introduce interventions by manipulating the Markov transition matrix for each individual, simulating shifts in personal location preferences. This is achieved by shuffling the empirical visit numbers for a group of locations, which maintains the overall number of visits while altering the choice probabilities for each location. The strength of the intervention is controlled by selecting the location group to include in the shuffling process.

For each intervention, the DT-EPR model generates interventional mobility trajectories $\tilde{T}^i = (L_k)_{k=1}^{m_{u^i}}$ for individual $u^i \in \mathcal{U}$, which share an identical data format as the observational mobility traces T^i .

3.3. Next location prediction networks

To assess the influence of causal interventions, i.e., the impact of changes in mobility behavior, we evaluate the predictive capabilities of a neural network trained on observational data but tested on interventional

data. We choose next location prediction as the application task. Practically, consider a sub-sequence $(L_k)_{k=m}^n \in T^i$ visited by individual u^i in a time window from time step m to n , the goal is to predict the location the same individual will visit in the next time step, i.e., the location identifier $l_{n+1} \in \mathcal{O}$. While conventional approaches to next location prediction relied on Markov models and matrix factorization methods, recent years have witnessed a growing adoption of neural networks (Luca et al., 2021). In the following, we present a typical pipeline for applying these networks to next location prediction, including generating feature embedding, designing the prediction network, and defining a loss function for parameter optimization.

An effective location prediction method starts by appropriately selecting and modeling the information in historical sequences. We include location identifiers, the time for location visits, and information regarding the individual who conducted the visit. To represent these features, we introduce embedding layers that utilize parameter matrices to map the original variables to real-valued embedding vectors. For each location L_k , vector representations of its location identifier l_k and time of arrival t_k are obtained as follows:

$$e_k^l = h^l(l_k; \mathbf{W}^l) \quad e_k^t = h^t(t_k; \mathbf{W}^t) \quad (4)$$

where e_k^l and e_k^t are the respective embedding vectors, $h(\cdot; \cdot)$ denotes the embedding operation, and \mathbf{W} terms are the learned parameter matrices during training. To capture different periodicity levels, we separately embed the minute, the hour, and the day of the week from the visit time t_k (Hong et al., 2022). The overall embedding vector e_k^{all} is obtained by adding the location and temporal embedding vectors: $e_k^{all} = e_k^l + e_k^t$. Additionally, we represent the individual u^i that conducted the travel into a vector e^{u^i} through a user embedding layer, i.e., $e^{u^i} = h^u(u^i; \mathbf{W}^u)$. Therefore, we obtain the overall embedding vector e_k^{all} that encodes spatiotemporal features at each time step and the user embedding vector e^{u^i} corresponding to each location sequence.

A location prediction network aims to learn the transition patterns between historical location visits in order to predict the next possible location. Without loss of generality, this process can be viewed as obtaining a (highly non-linear) mapping g with learnable parameters \mathbf{W}^g between the visit sequence $(e_k^{all})_{k=m}^n$, user information e^{u^i} and the ground-truth next location l_{n+1} , i.e., $l_{n+1} = g((e_k^{all})_{k=m}^n, e^{u^i}; \mathbf{W}^g)$. When a new visit sequence is observed, the mapping g is used to infer the predicted next location \hat{l}_{n+1} . Various sequential modeling methods can be employed to approximate g , among which Long Short-Term Memory (LSTM) (Hochreiter and Schmidhuber, 1997) and Multi-Head Self-Attention (MHSA)-based (Vaswani et al.,

2017) networks have gained considerable attention in the field (Luca et al., 2021). We implement the LSTM and MHSA-based networks for predicting the next location, and refer readers to Solomon et al. (2021) and Hong et al. (2022) for their detailed implementations, respectively.

In practice, for efficient parameter optimization, the prediction network outputs a visiting probability for each location instead of directly predicting the exact next location:

$$P(\hat{l}_{n+1}) = \text{Softmax}(g((e_k^{all})_{k=m}^n, e^{u^i}; \mathbf{W}^f)) \quad (5)$$

where $P(\hat{l}_{n+1}) \in [0, 1]^{|C|}$ contains the visit probabilities of all locations at the next time step, and Softmax denotes the softmax operation, ensuring $P(\hat{l}_{n+1})$ is a valid probability distribution. With access to the ground truth next location l_{n+1} during training, we can regard it as a multi-class classification problem, such that the network can be optimized using the multi-class cross-entropy loss \mathcal{L} :

$$\mathcal{L} = - \sum_{k=1}^{|C|} P(l_{n+1})^{(k)} \log(P(\hat{l}_{n+1})^{(k)}) \quad (6)$$

where $P(\hat{l}_{n+1})^{(k)}$ represents the predicted probability of visiting the k -th location (the k -th entry in $P(\hat{l}_{n+1})$) and $P(l_{n+1})^{(k)}$ is the one-hot represented ground truth, i.e., $P(l_{n+1})^{(k)} = 1$ if and only if the k -th location corresponds to the ground truth next location.

4. Data set and Experiment

4.1. Movement data and preprocessing

Individual mobility models rely on behavioral parameters calibrated from empirical tracking records to ensure a realistic representation of mobility behavior. To estimate these parameters characterizing individual mobility, we leverage a large-scale longitudinal GNSS tracking data set from the SBB Green Class (GC) E-Car pilot study conducted by the Swiss Federal Railways (SBB). The pilot study aimed to assess the impact of a Mobility-as-a-Service (MaaS) offer on mobility behavior (Martin et al., 2019). The study involved 139 participants based in Switzerland from November 2016 to December 2017. As part of the data collection process, participants were asked to install a commercial application (app) on their smartphones, which continuously recorded their whereabouts from GNSS signals. By analyzing motion measurements such as speed and acceleration, the app pre-processed the raw traces to identify two types of mobility events: *stay points* representing areas where users were stationary, and *stages* representing continuous movements using

a single travel mode.

We perform a series of preprocessing steps on the GC data set. First, to ensure high-quality tracking data for analysis, we include participants with extended tracking periods (observed for more than 300 days) and high temporal tracking coverage (whereabouts known for more than 60% of the time). Then, locations, serving as the basic movement units in individual mobility models, are derived from stay point sequences. We identify *activities* from stay points with durations exceeding 25 minutes. Locations are formed by aggregating activity stay points spatially: we use the DBSCAN clustering algorithm with parameters $\epsilon = 20$ and $num_samples = 1$ from the *Trackintel* library to generate *data set*-level locations (Martin et al., 2023a).

4.2. Realization of mobility models

The preprocessed GC data set is used to estimate the parameters of individual mobility models, including the jump length distribution $P(\Delta r)$ for vanilla EPR, as well as the waiting time distribution $P(\Delta t)$ and distributions for exploration tendency ($P(\rho)$ and $P(\gamma)$) for EPR-like models. Specifically, we consider the log-normal distribution and the power law (including truncated power law) distribution as candidate distributions for determining $P(\Delta r)$ and $P(\Delta t)$ (Alessandretti et al., 2017). We use the functions provided by the *powerlaw* library (Alstott et al., 2014) and evaluate the goodness-of-fit using the Akaike information criterion (AIC) and Akaike weights (Zhao et al., 2015). Under AIC, both distributions are best fitted using a log-normal distribution of the probability density function $P(x) = \frac{1}{x\sigma\sqrt{2\pi}} \exp\left(-\frac{(\ln(x)-\mu)^2}{2\sigma^2}\right)$ with parameters $\mu|_{\Delta r} = 7.72$, $\sigma|_{\Delta r} = 2.38$, and $\mu|_{\Delta t} = 0.75$, $\sigma|_{\Delta t} = 1.49$, respectively. To estimate the exploration tendencies $P(\rho)$ and $P(\gamma)$, we calculate the location exploration speed for GC individuals and fit normal distributions across individuals. We obtain $\mu|_{\rho} = 0.18$, $\sigma|_{\rho} = 0.07$ and $\mu|_{\gamma} = 0.64$, $\sigma|_{\gamma} = 0.16$, respectively. These values are consistent with the numbers presented in Song et al. (2010a).

We simulate mobility traces for 800 individuals in the observational data set as well as in each interventional data set using the DT-EPR process (see Section 3.1). For each synthetic individual, we independently sample ρ and γ from the distributions $P(\rho)$ and $P(\gamma)$, respectively. Individuals are randomly assigned to start at one of their top-5 visited locations, which are empirically observed from GC. The generation process continues until individuals have visited 2000 locations, which approximately matches the tracking length of the GC study.

After obtaining observational location sequences T^i and interventional location sequences \tilde{T}^i , we compare their mobility behaviors using mobility metrics:

- The real entropy (Song et al., 2010b) quantifies the regularity of location visit sequences by considering

the order and frequency of location visits. It provides insights into the theoretical predictability of individual mobility (Hong et al., 2023b).

- The mobility motifs (Schneider et al., 2013) refer to recurring sub-structures that arise when representing daily location visits of individuals as graphs. These motifs represent common mobility patterns shared among users, and the proportion of motifs for an individual reflects the prevalence of these shared patterns (Cao et al., 2019).

We present additional metrics, including radius of gyration (González et al., 2008), number of transited location pairs (Zhao et al., 2021), and location visitation frequency (González et al., 2008), in Appendix A.

4.3. Implementation of prediction networks

Next location prediction networks consider the past seven days as historical length; that is, the goal is to predict the following location an individual will be visiting based on their mobility history in the previous seven days. We adopt a common problem formulation, where prior mobility knowledge is assumed to be available for each individual. Hence, we partition each data set (i.e., observational and interventional) into non-overlapping train, validation, and test sets based on time. The splitting ratio is set to 3:1:1, where locations occurring in the first 60% of days for each individual are assigned to the train set, and the last 20% are assigned to the test set. We utilize the observational training set to optimize network parameters, and the corresponding validation set to monitor the network loss and performance during training. We conduct a grid search to find the optimal hyper-parameters that minimize the network loss on the same validation set. The considered hyper-parameters, the search ranges, and the final selected values can be found in Appendix B. Finally, we evaluate the performances of the networks using the held-out test sets from observational and interventional traces.

During training, we minimize Eq. 6 with the Adam optimizer (Kingma and Ba, 2015) on batches of training data samples. The initial learning rate is set to $1e^{-3}$, and an L2 penalty of $1e^{-6}$ is applied to the network loss. We adopt an early stopping strategy, which drops the learning rate by 0.1 if the validation loss does not decrease for 3 consecutive epochs. This early stopping process is repeated 3 times. After training, we evaluate the location prediction performances using a set of commonly applied metrics:

- Accuracy@k (Acc@k) measures the correctness by checking if the ground truth location is among the top- k most likely visited locations predicted by the network (in $P(\hat{l}_{n+1})$ from Eq. 5). We report Acc@1, Acc@5, and Acc@10.

- F1 score (F1) calculates the harmonic mean of precision and recall, considering the uneven visitation preferences to locations in daily routines. We utilize an F1 score weighted by the visit frequency to emphasize the performance in predicting important locations.
- Mean reciprocal rank (MRR) assesses the relevance of the recommended locations and is defined as the average reciprocal rank at which the ground truth location is identified by the network (in $P(\hat{l}_{n+1})$ from Eq. 5).

5. Results

5.1. Mobility simulation and intervention

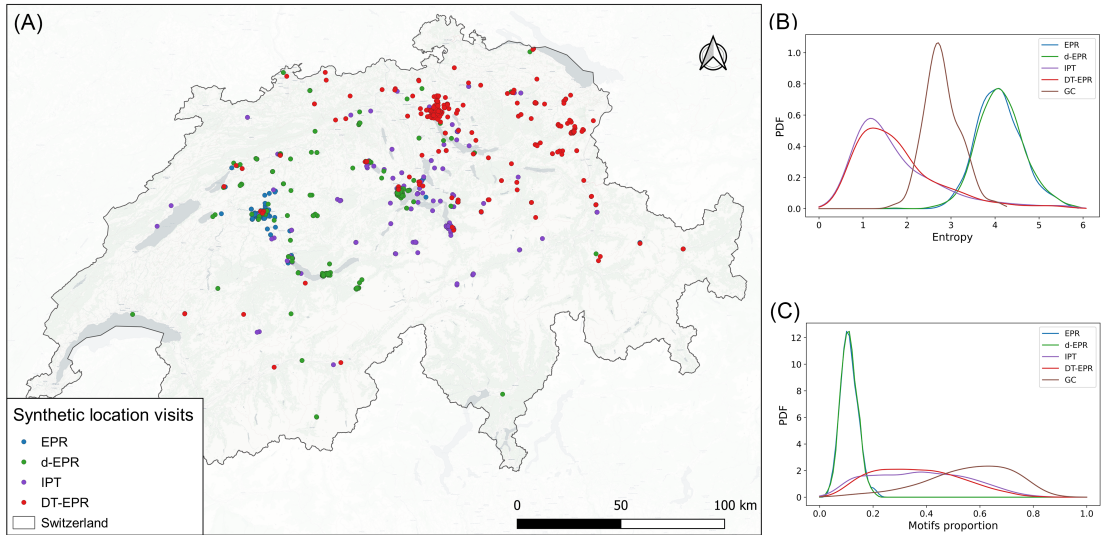


Figure 3: Synthetic location visits generated by EPR-like individual mobility models. (A) Spatial distribution of location visits for an exemplary user. (B) Mobility entropy and (C) motifs proportion distributions of the generated population. Map data ©OpenStreetMap contributors, ©CARTO.

By leveraging generative models and empirically estimating their behavior parameters, we obtain location traces for a set of synthetic individuals. The generation result is illustrated in Figure 3, where we map a selected individual’s locations and plot the entropy and motifs proportion measures for the entire data set. The spatial distribution of location visits (Figure 3A) clearly shows the patterns exhibited by EPR-like models. The vanilla EPR model assigns visit probabilities based solely on the geographical distance, thus generating location visits that are clustered around a central area. While the traces obtained from a d-EPR model are more concentrated in large cities, the locations generated by an IPT model are more dispersed in space, reflecting the empirical knowledge of that specific individual. Finally, the DT-EPR model combines

the advantages of both d-EPR and IPT models, producing traces that prioritize locations within urban areas (population attractiveness) and occasionally occur in distant sites (personal preferences). Furthermore, we quantitatively assess the regularities of the generated sequences at the data set level (Figure 3B and C). EPR and d-EPR exhibit the highest entropy and lowest motifs proportion among all mobility models, indicating that their location visit patterns are irregular and hard to predict. Although the d-EPR model introduces population attractiveness in the exploration phase, it does not alter the process of visiting known locations, which is the primary mechanism underlying mobility’s regularity. On the contrary, DT-EPR incorporates the first-order Markov dependence on location visits, producing the most regular location visitation patterns, as evidenced by the lowest entropy and highest motif proportion distributions among all models. Another intriguing observation arises when comparing the distributions of the generated traces with those from the real data. The result from DT-EPR displays lower entropy, signifying higher regularity in location visits, but generally has a lower motifs proportion compared to the real traces (labeled as GC in Figure 3B and C).

Next, we introduce causal interventions to the data-generation process. The direction and impact of these interventions on mobility behavior are assessed using a comprehensive set of mobility metrics. Figure 4 displays the distributions of mobility entropy and motifs proportion for both observational and interventional location sequences from DT-EPR. The latter are generated by implementing various interventions on individuals’ exploration tendencies. Additional metrics for describing the impact of these interventions can be found in Appendix A. The interventions on population-level attractiveness and individual-level preference preserve the general visitation characteristics; hence, high-level mobility metrics cannot accurately reflect their impact.

The introduced causal intervention can effectively and directionally change the underlying mobility pattern, as demonstrated in Figure 4. The strength of the intervention is evaluated by examining the extent of distribution shifts in the mobility metrics. For example, with an increase in the exploration tendency p^{new} , individuals are encouraged to visit new locations, resulting in an increasingly higher number of transited location pairs (Appendix A) and leading to mobility sequences with higher entropy and lower motifs proportion (Figure 4A). Moreover, the impact on the generated location sequences can be compared among the different interventions. While intervening on the exploration tendency p^{new} significantly alters the mobility patterns (Figure 4A), changes induced by exploration parameters ρ and γ are more nuanced and provide more fine-grained control (Figure 4B and C). In summary, mobility metrics facilitate the description and comparison between observational and interventional location sequences, allowing us to assess the direction

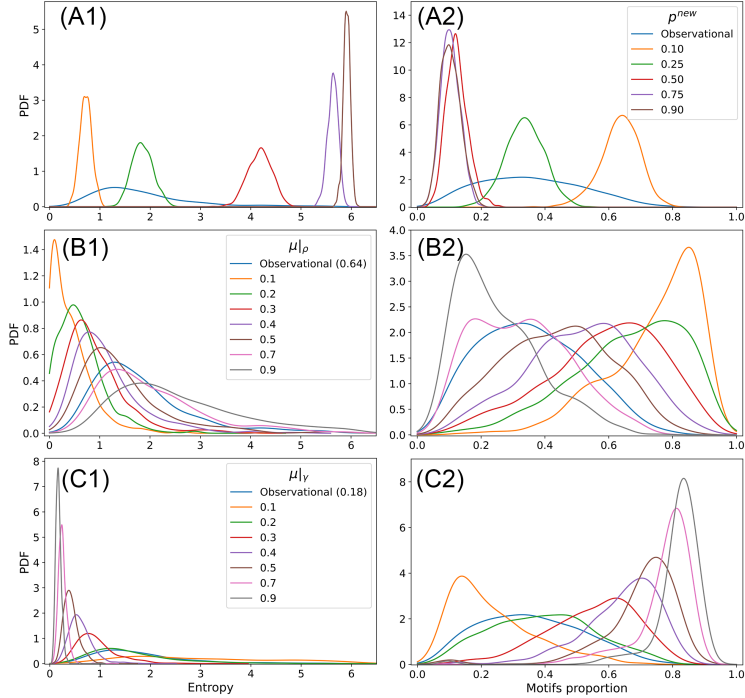


Figure 4: The entropy and motifs proportion distributions of observational and interventional location sequences. We show the metric distributions for (A) hard interventions on p^{new} , (B) interventions on ρ by shifting $\mu|_{\rho}$ of $P(\rho)$, and (C) interventions on γ by shifting $\mu|_{\gamma}$ of $P(\gamma)$.

and strength of the interventions on mobility behavior.

5.2. Next location prediction

Thanks to the individual mobility simulation models and the causal intervention process, we can assess the performance of predictive networks when confronted with distribution shifts. We begin by comparing the location prediction performance of LSTM and MHSA on mobility sequences generated by different variants of the EPR model (Table 1), thereby uncovering the influence of generative mechanisms. These networks are trained with location sequences from DT-EPR and evaluated on data sets obtained using the same observational parameters but different ablations of its components. We also assess their performances on a new DT-EPR population with different initializations (e.g., for each individual a newly sampled start location, ρ , and γ ; see Section 4.2 for details of the mobility model realization). This variant is denoted as *DT-EPR re-generated* in Table 1, with the network performance differences reflecting the effect of induced randomness in the mobility model. When evaluated on the training population (*DT-EPR trained* in Table 1), MHSA demonstrates a stronger capability to correctly infer the next location compared to LSTM, as indicated by the higher performance indicators Acc@1, F1, and MRR. However, LSTM outperforms

MHSA when confronted with all other populations, i.e., when predicting for location sequences on which the network was not trained, demonstrating superior generalization ability. In addition, both networks exhibit the worst performance when provided with sequences obtained from the vanilla EPR model, indicating the absence of clear transition patterns in these sequences – a property overlooked by the EPR mechanism. As a further enhancement to the model, IPT enables the generation of location sequences with transition patterns that a predictive network can utilize for inferring the next location. Moreover, incorporating population preferences during exploration imposes essential structural patterns in location visit sequences, as evidenced by the increase in prediction performance between EPR and d-EPR, as well as IPT and DT-EPR. These structural patterns are not apparent in the entropy and motifs proportion distributions (Figure 3), yet, they contribute to increasing the accuracy of next location prediction (Table 1).

Table 1: Next location prediction performances for observational location sequences from EPR-like models. The mean and standard deviation across five runs with different random parameter initializations are reported.

Networks	Data sets	Acc@1	Acc@5	Acc@10	F1	MRR
LSTM	EPR	1.1 ± 0.03	2.8 ± 0.04	3.9 ± 0.02	0.3 ± 0.01	2.2 ± 0.03
	d-EPR	1.2 ± 0.04	3.2 ± 0.1	4.6 ± 0.1	0.4 ± 0.04	2.5 ± 0.05
	IPT	17.3 ± 0.3	25.8 ± 0.3	28.8 ± 0.2	11.2 ± 0.1	21.4 ± 0.2
	DT-EPR re-generated	25.1 ± 0.2	35.1 ± 0.2	38.5 ± 0.2	17.8 ± 0.2	30.0 ± 0.2
	DT-EPR trained	55.0 ± 0.1	62.9 ± 0.1	64.6 ± 0.05	46.2 ± 0.2	58.6 ± 0.1
MHSA	EPR	0.8 ± 0.01	2.4 ± 0.02	3.7 ± 0.02	0.3 ± 0.01	2.0 ± 0.01
	d-EPR	0.9 ± 0.01	2.8 ± 0.02	4.2 ± 0.04	0.4 ± 0.01	2.2 ± 0.01
	IPT	15.0 ± 0.2	23.7 ± 0.4	27.3 ± 0.4	10.6 ± 0.1	19.3 ± 0.2
	DT-EPR re-generated	24.4 ± 0.1	33.8 ± 0.2	37.5 ± 0.2	18.7 ± 0.04	29.0 ± 0.1
	DT-EPR trained	55.8 ± 0.02	62.7 ± 0.04	64.4 ± 0.03	47.3 ± 0.04	59.1 ± 0.02

5.3. Robustness of location prediction networks

We now evaluate the performance of networks using the interventional mobility sequences, which reveals the network robustness in OoD scenarios, i.e., when the training and testing data are not generated from the same underlying distribution. Figure 5 displays the variations in Acc@1 and MRR scores of the LSTM and MHSA networks for interventions on exploration tendency, and Figure 6 depicts the same performance variation plot for interventions on population attractiveness and individual preference. The complete performance results for all conducted interventions are presented in Appendix C. The prediction networks remain consistent with those described in the previous section, i.e., they are trained using observational location sequences from DT-EPR. Consequently, the performance metrics in OoD scenarios can be cross-compared with those presented in Table 1. Although similar performance trends are observed for both networks, LSTM consistently outperforms MHSA in OoD settings, confirming the observation from the previous results.

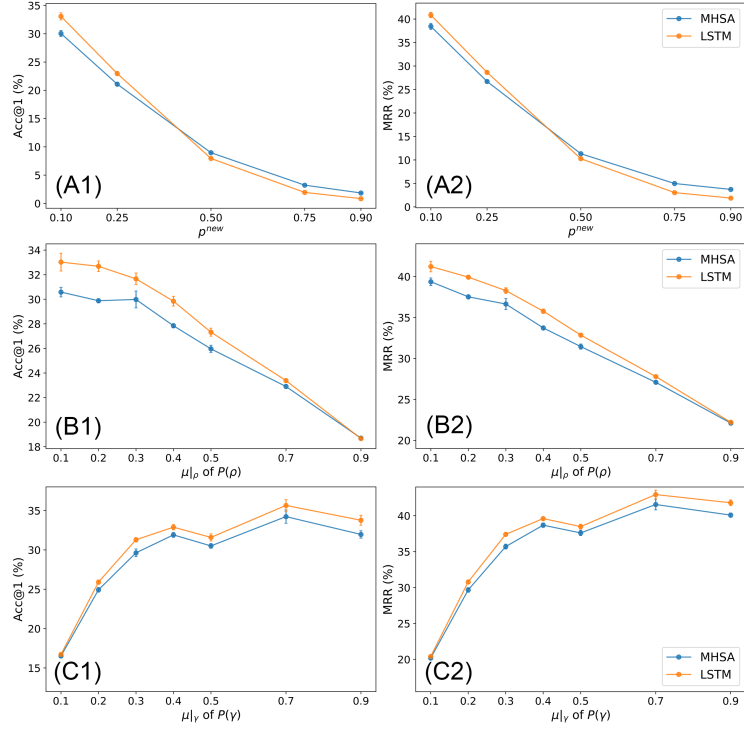


Figure 5: Next location prediction performances for interventions on individuals' exploration tendency. We show the variations in Acc@1 and MRR for (A) hard interventions on p^{new} , (B) interventions on ρ by shifting $\mu|_{\rho}$ of $P(\rho)$, and (C) interventions on γ by shifting $\mu|_{\gamma}$ of $P(\gamma)$. Error bars indicate the standard deviation across five different runs.

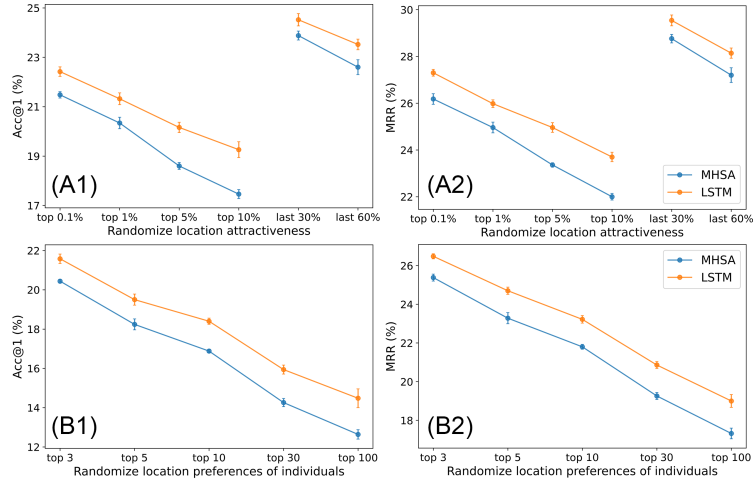


Figure 6: Next location prediction performances for interventions on population attractiveness and individual preference. We show the variations in Acc@1 and MRR for (A) randomizing empirical location visits of the data set, and (B) randomizing empirical location visits for each individual. Error bars indicate the standard deviation across five different runs.

The performance variations for different exploration interventions (Figure 5) generally align with their strengths and directions, as measured using mobility metrics shown in Figure 4. We also observe non-linear relations between intervention strength and prediction performance. In particular, the hard interventions on

p^{new} significantly influence the prediction capability. Setting $p^{new} > 0.5$ results in performance indicators of $\text{Acc}@1 < 10\%$ and $\text{MRR} < 10\%$, suggesting that the learned location transition patterns cannot be adequately utilized. Comparatively, interventions on γ and ρ indirectly affect p^{new} , which retains the diminishing exploration speed over time. As a result, the influences on the performance for next location prediction are milder, e.g., the $\text{Acc}@1$ still achieves $\sim 18\%$ with the strongest implemented interventions ($\mu|_{\rho} = 0.9$ and $\mu|_{\gamma} = 0.1$). Moreover, we observe the prediction performances are relatively stable for $\mu|_{\rho} \in [0.1, 0.3]$ and $\mu|_{\gamma} \in [0.5, 0.9]$, even though the location sequences continue to exhibit lower mobility entropy and higher motifs proportion (Figure 4) due to decreasing exploration tendency. This saturation suggests that even if individuals explore new locations at a lower rate, many location visit patterns are inherently stochastic and complex, making them challenging to capture by a trained network.

Interventions on population attractiveness and individual preference reveal how altering visit frequencies for specific locations affects the prediction performances, as shown in Figure 6. In each intervention, we consider a set of locations and randomly shuffle their empirical visitation numbers within the group; for instance, in the shuffling process, “top 1%” includes the most frequently visited 1% of locations across the population (Figure 6A), and “top 3” considers the three most visited locations for each individual (Figure 6B). Both types of interventions substantially impact the ability to correctly predict the next location, with altering the number of visits separately for each individual showing a stronger influence, as evidenced by the higher drop in performance indicators. When compared with the observational data sets (Table 1), even changes in preference for a few most critical locations (e.g., “top 0.1%” for location attractiveness or “top 3” for individual preferences) result in a significant prediction capability decrease. On the contrary, intervening on a large portion of locations that are not frequently visited (i.e., “last 30%” and “last 60%” for location attractiveness) has minimal impact on the prediction performances. These results emphasize the indispensable role of essential locations in shaping daily mobility and reveal their relation with the generalization ability of next location prediction networks.

6. Discussion

This study has assessed the robustness of neural networks on the next location prediction task. We implement both conventional and contemporary individual mobility simulation models, on which we conduct causal interventions to simulate mobility traces when structural changes occur. These interventional mobility traces are then used as input for trained networks and evaluated for location prediction. The examination of mobility simulators revealed that the vanilla EPR mechanism fails to simulate sequences with realistic

visitation order despite its ability to reproduce scaling laws of location visits (Figure 3 and Table 1). In contrast, although IPT explicitly incorporates the first-order Markov dependence in the generation process, it tends to produce over-regular sequences (Figure 3B) and lacks the representation of higher-order patterns in daily mobility (Figure 3C). These findings highlight the need for further developments in individual mobility simulation models, essential for visit order-sensitive applications, such as mobility prediction (Ma and Zhang, 2022) and smart charging optimization (Cai et al., 2022). Moreover, the comparison between the two sequence modeling networks, LSTM and MHSA-based, reveals their generalization characteristics. While the MHSA-based network performs better when predicting locations for the same population, LSTM demonstrates higher generalization capability when dealing with sequences sampled OoD.

Performing causal interventions on the mobility simulators enables us to control the strength and direction of mobility behavior. These interventions not only quantitatively reveal the impacts of behavior on location predictors but also have critical practical implications for downstream applications. In particular, we analyze how changes in exploration tendency, a fundamental property of human mobility, affect location prediction network performances. Thanks to the high-level mobility metrics, we establish a link between exploration tendency, mobility behavior, and prediction performance, providing a benchmark for cross-comparing existing or newly developed individual mobility prediction networks, possibly implemented on other data sets. This allows studies to evaluate the mobility behavior of their population, and assess whether their networks achieve increased performance compared to the numbers reported in this study. Furthermore, the performance quantification for specific mobility patterns aids in selecting populations for developing predictive networks or preemptively evaluating the performances of demographic groups (Baumann et al., 2018).

Additionally, the interventions on location preferences simulate spatiotemporal shifts in mobility behavior. The introduced preference interventions heavily influence the performance of prediction networks. Nevertheless, these interventions are hardly distinguishable from the observational ones with high-level mobility metrics, as these interventions alter location choices while maintaining the empirical visitation distribution. This highlights the importance of developing change detection methods that are able to delineate these fine-grained mobility behavior change points or periods (Hong et al., 2021). Moreover, the impact of interventions on location prediction reveals that preference changes in the essential locations have a much more significant effect on the prediction network than changes in the less visited ones. However, recent studies on intra-person variability of travel behavior suggest that individuals constantly update their important locations over time (Alessandretti et al., 2018), implying real-world deployment of mobility prediction

networks requires the integration of online learning, where networks are continuously updated as new data arrives (Jiang et al., 2018). In this online learning framework, this study can assist in identifying the time point when the performance of the network is no longer sufficient and subsequently perform the parameter update to adapt to the evolving mobility behavior.

7. Conclusion

Unraveling the role and impact of multifaceted mobility behavior on prediction outcomes is imperative to the real-world application of mobility prediction systems. Here, we present a framework to examine how behavioral factors influence mobility prediction networks through causal interventions. We achieve this by utilizing individual mobility models, wherein parameters capture various aspects of mobility behaviors. We perform causal interventions on these parameters to generate individual mobility traces that mirror realistic real-world variations in behavior. Quantitative evaluation using mobility metrics demonstrates our capability to effectively and deliberately modify mobility behaviors by controlling the intervention strength. Subsequently, we evaluate these interventional traces with well-trained networks for the next location prediction task, and the resulting performance variations indicate the robustness of networks when facing domain shifts. Our results reveal vital behavior factors affecting prediction performance, including sequential location transition patterns, the tendency to explore new locations, and location preferences at both population and individual levels. These findings demonstrate the effectiveness of the framework, and pave the way for various downstream applications, including cross-comparisons among prediction networks and performance monitoring in dynamically evolving spatiotemporal scenarios.

As one of the pioneering studies to explore the causal impact of mobility behavior on individual mobility prediction, this research sheds light on several directions for future work. The proposed framework is applicable to any mechanistic generation model that can be abstracted as an SCM. While our designed interventions and analysis are rooted in the mechanism employed by the EPR model and its extensions, future studies should explore other mobility simulation models, such as location attractiveness (Yan et al., 2017) and container (Alessandretti et al., 2020), to examine the impact of alternative behavior mechanisms on mobility prediction. In addition to factors that describe mobility, quantifying the causal effects of contexts (e.g., urban functions, land use, and weather situations) on mobility behavior is a direction worth exploring. This endeavor would require a mechanistic model that explicitly formulates the relationship between contextual factors and mobility behavior, which could be inferred with the use of causal discovery methods (Runge et al., 2023). Last, counterfactuals offer greater causal reasoning capabilities than interventions, as outlined

in the three-layer causal hierarchy of association (layer 1), intervention (layer 2), and counterfactual (layer 3) by Pearl and Mackenzie (2018). Exploring counterfactual explanations for prediction networks provides actionable suggestions that can lead to desirable alternative outcomes (Xin et al., 2022). This aspect is crucial for the real-world deployment of mobility prediction systems, even though its full potential remains to be fully realized. In conclusion, we expect this study to stimulate innovative approaches that leverage causal inference to improve the interpretability and robustness of neural networks when applied to mobility analysis and prediction.

Appendix

A. Additional metrics for describing mobility behavior

Apart from the mobility metrics elucidated in the main text, we introduce additional metrics to characterize mobility behavior within both observational and interventional location visitation sequences:

- The radius of gyration (González et al., 2008) measures the characteristic distance traveled by an individual and is commonly used to reflect their movement intensity in the spatial dimension. Its data set distribution reveals the heterogeneity level in user movement (Xu et al., 2018a).
- The number of transited location pairs (Zhao et al., 2021) measures the number of links in an individual mobility graph, where locations are represented as nodes and travels between locations are represented as edges.
- The location visitation frequency distribution (González et al., 2008) is known to adhere to Zipf’s law, where individuals tend to spend the majority of their time at a small number of frequently visited locations. The exponent of this power law, which characterizes the shape of the distribution, reveals the frequency of important location visits and can serve as an indicator of mobility regularity.

Figure S1 illustrates alterations in mobility patterns resulting from interventions on the exploration behavior, assessed using the previously mentioned metrics. Notably, these interventions induced changes in the population’s mobility intensity, quantified by the radius of gyration. Although these interventions had a marginal impact on the prevalence of individuals traveling shorter distances, they substantially reduced the likelihood of encountering individuals with extensive travel patterns as exploration declined (lower p^{new} and $\mu|_{\rho}$, and higher $\mu|_{\gamma}$). As expected, a reduction in exploration inclination led to fewer transited location pairs per day (Figure S1 middle panel) and a significant decrease in the visitation frequency of the most frequently visited locations (Figure S1 right panel).

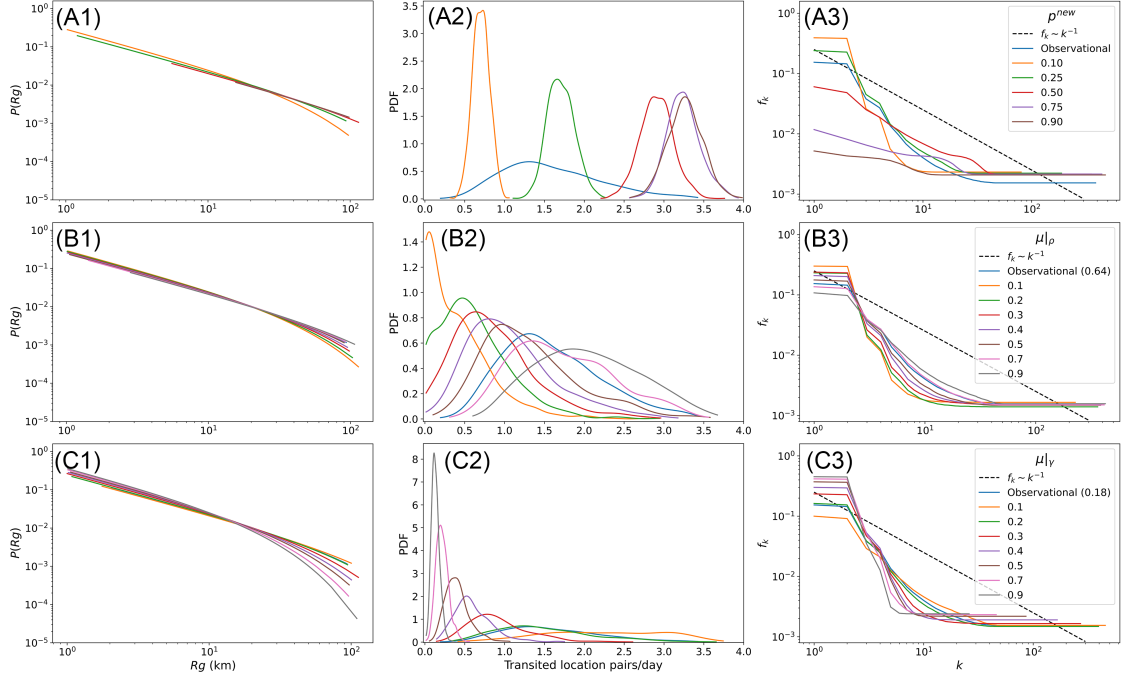


Figure S1: The radius of gyration (R_g), number of transited location pairs, and location visitation frequency distributions of observational and interventional location sequences. We show the metric distributions for (A) hard interventions on p^{new} , (B) interventions on ρ by shifting $\mu|_{\rho}$ of $P(\rho)$, and (C) interventions on γ by shifting $\mu|_{\gamma}$ of $P(\gamma)$.

B. Hyper-parameter search for prediction networks

We use a batch size of 256 for training the LSTM and MHSA-based networks. Zeros are appended to the end of each input sequence until its length matches that of the longest sequence, ensuring consistent length within each batch. The tuned hyper-parameters and their search ranges are shown in Table S1. We determine the optimal set of values as the one that minimizes the network loss on the validation set of the observational traces from DT-EPR.

Table S1: Hyper-parameter search for next location prediction networks.

	Hyper-parameter	Search range	Optimal value
LSTM	Embedding dim.	{32, 64, 128}	64
	Hidden dim.	{64, 128, 256, 512}	128
MHSA-based	#Heads	{2, 4, 8}	8
	#Layers	{2, 4, 6}	4
	Embedding dim.	{32, 64, 128}	64
	Feed-forward dim.	{64, 128, 256, 512}	256

C. Network performances on interventional location sequences

The complete performance evaluation results for LSTM and MHSA-based networks on all generated interventional location sequences are presented in Table S2 and Table S3, respectively. We report the mean and standard deviation across five network optimization runs with different random parameter initializations.

Table S2: Performance of the LSTM model in predicting the next location on interventional location sequences.

Intervention	Strength	Acc@1	Acc@5	Acc@10	F1	MRR
p^{new}	0.1	33.0 ± 0.6	49.8 ± 0.6	55.3 ± 0.6	28.9 ± 0.5	40.8 ± 0.6
	0.25	23.0 ± 0.3	34.8 ± 0.1	38.7 ± 0.1	16.2 ± 0.1	28.6 ± 0.3
	0.5	7.9 ± 0.1	12.4 ± 0.03	14.4 ± 0.05	3.6 ± 0.1	10.3 ± 0.04
	0.75	1.9 ± 0.1	3.7 ± 0.1	4.9 ± 0.1	0.6 ± 0.04	3.0 ± 0.1
	0.9	0.9 ± 0.04	2.3 ± 0.1	3.5 ± 0.1	0.3 ± 0.03	1.9 ± 0.1
$\mu _{\rho}$	0.1	33.0 ± 0.7	50.7 ± 0.7	56.5 ± 0.4	29.2 ± 0.6	41.2 ± 0.7
	0.2	32.7 ± 0.4	48.0 ± 0.3	53.0 ± 0.6	28.3 ± 0.3	39.9 ± 0.2
	0.3	31.7 ± 0.5	45.8 ± 0.4	50.4 ± 0.3	25.9 ± 0.4	38.3 ± 0.3
	0.4	29.8 ± 0.4	42.4 ± 0.4	47.1 ± 0.3	23.5 ± 0.4	35.8 ± 0.3
	0.5	27.3 ± 0.3	38.9 ± 0.3	42.9 ± 0.2	20.5 ± 0.3	32.8 ± 0.2
	0.7	23.4 ± 0.1	32.4 ± 0.1	35.7 ± 0.1	16.2 ± 0.1	27.8 ± 0.1
	0.9	18.6 ± 0.05	25.8 ± 0.1	28.3 ± 0.1	11.5 ± 0.2	22.2 ± 0.1
$\mu _{\gamma}$	0.1	16.7 ± 0.1	24.2 ± 0.1	26.9 ± 0.1	10.2 ± 0.1	20.4 ± 0.1
	0.2	25.9 ± 0.3	36.0 ± 0.2	39.4 ± 0.3	18.6 ± 0.2	30.8 ± 0.2
	0.3	31.3 ± 0.3	44.2 ± 0.2	48.2 ± 0.6	24.8 ± 0.1	37.4 ± 0.2
	0.4	32.9 ± 0.4	47.1 ± 0.2	51.7 ± 0.2	27.1 ± 0.2	39.6 ± 0.3
	0.5	31.6 ± 0.4	46.3 ± 0.4	51.2 ± 0.3	26.9 ± 0.5	38.5 ± 0.3
	0.7	35.6 ± 0.7	51.4 ± 0.4	56.7 ± 0.7	31.6 ± 0.7	42.9 ± 0.6
	0.9	33.8 ± 0.6	51.2 ± 0.5	57.0 ± 0.9	30.0 ± 0.5	41.8 ± 0.4
Attractiveness	top 0.1%	22.4 ± 0.2	32.6 ± 0.2	35.8 ± 0.2	15.5 ± 0.3	27.3 ± 0.1
	top 1%	21.3 ± 0.2	30.9 ± 0.1	34.4 ± 0.2	14.6 ± 0.1	26.0 ± 0.1
	top 5%	20.2 ± 0.2	30.1 ± 0.3	33.4 ± 0.1	13.5 ± 0.2	25.0 ± 0.2
	top 10%	19.3 ± 0.3	28.4 ± 0.2	31.5 ± 0.2	12.6 ± 0.2	23.7 ± 0.2
	last 30%	24.5 ± 0.3	35.0 ± 0.1	38.5 ± 0.1	17.5 ± 0.2	29.5 ± 0.2
	last 60%	23.5 ± 0.2	33.1 ± 0.3	36.3 ± 0.1	16.5 ± 0.1	28.1 ± 0.2
Preference	top 3	21.6 ± 0.2	31.7 ± 0.2	35.4 ± 0.1	14.9 ± 0.2	26.5 ± 0.2
	top 5	19.5 ± 0.3	30.4 ± 0.2	34.1 ± 0.2	13.5 ± 0.2	24.7 ± 0.2
	top 10	18.4 ± 0.2	28.3 ± 0.3	31.8 ± 0.4	12.5 ± 0.1	23.2 ± 0.2
	top 30	15.9 ± 0.3	26.2 ± 0.2	29.8 ± 0.3	10.7 ± 0.2	20.9 ± 0.2
	top 100	14.5 ± 0.5	23.7 ± 0.3	27.2 ± 0.3	9.4 ± 0.3	19.0 ± 0.3

Table S3: Performance of the MHSA model in predicting the next location on interventional location sequences.

Intervention	Strength	Acc@1	Acc@5	Acc@10	F1	MRR
p^{new}	0.1	30.0 ± 0.5	48.0 ± 0.9	54.2 ± 0.8	26.6 ± 0.3	38.4 ± 0.7
	0.25	21.1 ± 0.3	32.7 ± 0.1	36.9 ± 0.2	16.1 ± 0.1	26.7 ± 0.2
	0.5	9.0 ± 0.04	13.3 ± 0.04	15.4 ± 0.03	5.3 ± 0.04	11.3 ± 0.04
	0.75	3.2 ± 0.03	6.2 ± 0.1	8.1 ± 0.1	1.5 ± 0.04	5.0 ± 0.04
	0.9	1.8 ± 0.04	4.9 ± 0.1	7.0 ± 0.1	0.9 ± 0.04	3.7 ± 0.1
$\mu _{\rho}$	0.1	30.6 ± 0.4	49.1 ± 0.6	55.8 ± 0.7	27.8 ± 0.4	39.4 ± 0.5
	0.2	29.9 ± 0.2	45.9 ± 0.3	51.9 ± 0.6	26.4 ± 0.02	37.5 ± 0.2
	0.3	30.0 ± 0.7	44.0 ± 0.5	48.9 ± 0.6	25.4 ± 0.6	36.7 ± 0.7
	0.4	27.8 ± 0.2	40.0 ± 0.3	45.2 ± 0.4	22.8 ± 0.2	33.7 ± 0.2
	0.5	25.9 ± 0.3	37.3 ± 0.5	41.6 ± 0.4	20.5 ± 0.2	31.5 ± 0.3
	0.7	22.9 ± 0.2	31.3 ± 0.3	34.9 ± 0.2	17.2 ± 0.2	27.1 ± 0.2
	0.9	18.7 ± 0.05	25.4 ± 0.2	28.1 ± 0.1	13.0 ± 0.04	22.1 ± 0.1
$\mu _{\gamma}$	0.1	16.5 ± 0.2	23.8 ± 0.1	26.8 ± 0.1	11.4 ± 0.2	20.2 ± 0.2
	0.2	24.9 ± 0.3	34.6 ± 0.3	38.3 ± 0.3	19.2 ± 0.2	29.6 ± 0.3
	0.3	29.6 ± 0.5	42.4 ± 0.1	46.9 ± 0.1	24.4 ± 0.5	35.7 ± 0.3
	0.4	31.9 ± 0.3	46.0 ± 0.4	51.1 ± 0.3	27.3 ± 0.2	38.7 ± 0.3
	0.5	30.5 ± 0.3	45.3 ± 0.4	50.7 ± 0.4	26.8 ± 0.2	37.6 ± 0.4
	0.7	34.2 ± 0.8	49.4 ± 0.7	55.3 ± 1.2	31.0 ± 0.7	41.6 ± 0.8
	0.9	32.0 ± 0.4	49.0 ± 0.6	55.5 ± 0.3	29.0 ± 0.4	40.1 ± 0.3
Attractiveness	top 0.1%	21.5 ± 0.2	31.2 ± 0.4	34.8 ± 0.3	16.0 ± 0.1	26.2 ± 0.2
	top 1%	20.3 ± 0.2	29.6 ± 0.3	33.2 ± 0.4	15.1 ± 0.2	24.9 ± 0.2
	top 5%	18.6 ± 0.1	28.3 ± 0.3	32.0 ± 0.3	13.5 ± 0.1	23.4 ± 0.1
	top 10%	17.4 ± 0.2	26.6 ± 0.1	30.4 ± 0.1	12.5 ± 0.1	22.0 ± 0.1
	last 30%	23.9 ± 0.2	34.1 ± 0.2	37.7 ± 0.2	18.3 ± 0.1	28.8 ± 0.2
	last 60%	22.6 ± 0.3	32.0 ± 0.3	35.6 ± 0.3	17.1 ± 0.2	27.2 ± 0.3
Preference	top 3	20.4 ± 0.1	30.4 ± 0.3	34.3 ± 0.3	15.4 ± 0.1	25.4 ± 0.2
	top 5	18.3 ± 0.3	28.5 ± 0.3	32.4 ± 0.2	13.7 ± 0.2	23.3 ± 0.3
	top 10	16.9 ± 0.1	26.7 ± 0.2	30.6 ± 0.2	12.3 ± 0.2	21.8 ± 0.1
	top 30	14.3 ± 0.2	24.5 ± 0.3	28.5 ± 0.1	10.5 ± 0.2	19.3 ± 0.2
	top 100	12.6 ± 0.3	22.1 ± 0.3	25.9 ± 0.3	9.2 ± 0.1	17.3 ± 0.3

References

- L. Alessandretti, P. Sapiezynski, S. Lehmann, and A. Baronchelli. Multi-scale spatio-temporal analysis of human mobility. *PLOS ONE*, 12(2):e0171686, 2017. doi:[10.1371/journal.pone.0171686](https://doi.org/10.1371/journal.pone.0171686).
- L. Alessandretti, P. Sapiezynski, V. Sekara, S. Lehmann, and A. Baronchelli. Evidence for a conserved quantity in human mobility. *Nature Human Behaviour*, 2(7):485–491, 2018. doi:[10.1038/s41562-018-0364-x](https://doi.org/10.1038/s41562-018-0364-x).
- L. Alessandretti, U. Aslak, and S. Lehmann. The scales of human mobility. *Nature*, 587(7834):402–407, 2020. ISSN 1476-4687. doi:[10.1038/s41586-020-2909-1](https://doi.org/10.1038/s41586-020-2909-1).
- J. Alstott, E. Bullmore, and D. Plenz. powerlaw: A Python Package for Analysis of Heavy-Tailed Distributions. *PLoS ONE*, 9(1):e85777, 2014. doi:[10.1371/journal.pone.0085777](https://doi.org/10.1371/journal.pone.0085777).
- K. W. Axhausen and T. Gärling. Activity-based approaches to travel analysis: conceptual frameworks, models, and research problems. *Transport Reviews*, 12(4):323–341, 1992. doi:[10.1080/01441649208716826](https://doi.org/10.1080/01441649208716826).
- H. Barbosa, M. Barthelemy, G. Ghoshal, C. R. James, M. Lenormand, T. Louail, R. Menezes, J. J. Ramasco, F. Simini, and M. Tomasini. Human mobility: Models and applications. *Physics Reports*, 734:1–74, 2018.
- P. Baumann, C. Koehler, A. K. Dey, and S. Santini. Selecting Individual and Population Models for Predicting Human Mobility. *IEEE Transactions on Mobile Computing*, 17(10):2408–2422, 2018. doi:[10.1109/TMC.2018.2797937](https://doi.org/10.1109/TMC.2018.2797937).
- D. Brockmann, L. Hufnagel, and T. Geisel. The scaling laws of human travel. *Nature*, 439(7075):462–465, 2006. doi:[10.1038/nature04292](https://doi.org/10.1038/nature04292).
- H. Cai, Y. Xin, H. Martin, and M. Raubal. Optimizing electric vehicle charging schedules based on probabilistic forecast of individual mobility. *AGILE: GIScience Series*, 3:3, 2022. doi:[10.5194/agile-giss-3-3-2022](https://doi.org/10.5194/agile-giss-3-3-2022).
- J. Cao, Q. Li, W. Tu, and F. Wang. Characterizing preferred motif choices and distance impacts. *PLOS ONE*, 14(4):e0215242, 2019. doi:[10.1371/journal.pone.0215242](https://doi.org/10.1371/journal.pone.0215242).
- C. Chen, J. Ma, Y. Susilo, Y. Liu, and M. Wang. The promises of big data and small data for travel behavior (aka human mobility) analysis. *Transportation Research Part C: Emerging Technologies*, 68:285–299, 2016. doi:[10.1016/j.trc.2016.04.005](https://doi.org/10.1016/j.trc.2016.04.005).
- M. C. González, C. A. Hidalgo, and A.-L. Barabási. Understanding individual human mobility patterns. *Nature*, 453(7196):779–782, 2008. doi:[10.1038/nature06958](https://doi.org/10.1038/nature06958).
- A. Graser, A. Jalali, J. Lampert, A. Weißenfeld, and K. Janowicz. Deep Learning From Trajectory Data: a Review of Deep Neural Networks and the Trajectory Data Representations to Train Them. In *Proceedings of the Workshop on Big Mobility Data Analytics (BMDA) co-located with EDBT/ICDT 2023 Joint Conference*, 2023.
- T. He, J. Bao, R. Li, S. Ruan, Y. Li, L. Song, H. He, and Y. Zheng. What is the Human Mobility in a New City: Transfer Mobility Knowledge Across Cities. In *Proceedings of the 2020 World Wide Web Conference on World Wide Web (WWW '20)*, pages 1355–1365, New York, NY, USA, 2020. ACM Press. doi:[10.1145/3366423.3380210](https://doi.org/10.1145/3366423.3380210).
- B. Hintermann, B. Schoeman, J. Molloy, T. Schatzmann, C. Tchervenkov, and K. W. Axhausen. The impact of COVID-19 on mobility choices in Switzerland. *Transportation Research Part A: Policy and Practice*, 169:103582, 2023. doi:[10.1016/j.tra.2023.103582](https://doi.org/10.1016/j.tra.2023.103582).
- S. Hochreiter and J. Schmidhuber. Long Short-Term Memory. *Neural Computation*, 9(8):1735–1780, 1997. doi:[10.1162/neco.1997.9.8.1735](https://doi.org/10.1162/neco.1997.9.8.1735).
- Y. Hong, Y. Xin, H. Martin, D. Bucher, and M. Raubal. A clustering-based framework for individual travel behaviour change detection. In *11th International Conference on Geographic Information Science - Part II (GIScience '21)*, volume 208, page 4, 2021. doi:[10.4230/LIPIcs.GIScience.2021.II.4](https://doi.org/10.4230/LIPIcs.GIScience.2021.II.4).

- Y. Hong, H. Martin, and M. Raubal. How do you go where? improving next location prediction by learning travel mode information using transformers. In *Proceedings of the 30th International Conference on Advances in Geographic Information Systems (SIGSPATIAL '22)*, 2022. doi:[10.1145/3557915.3560996](https://doi.org/10.1145/3557915.3560996).
- Y. Hong, H. Martin, Y. Xin, D. Bucher, D. J. Reck, K. W. Axhausen, and M. Raubal. Conserved quantities in human mobility: From locations to trips. *Transportation Research Part C: Emerging Technologies*, 146:103979, 2023a. doi:[10.1016/j.trc.2022.103979](https://doi.org/10.1016/j.trc.2022.103979).
- Y. Hong, Y. Zhang, K. Schindler, and M. Raubal. Context-aware multi-head self-attentional neural network model for next location prediction. *Transportation Research Part C: Emerging Technologies*, 156:104315, 2023b. doi:[10.1016/j.trc.2023.104315](https://doi.org/10.1016/j.trc.2023.104315).
- X. Huang, D. Kroening, W. Ruan, J. Sharp, Y. Sun, E. Thamo, M. Wu, and X. Yi. A survey of safety and trustworthiness of deep neural networks: Verification, testing, adversarial attack and defence, and interpretability. *Computer Science Review*, 37:100270, 2020.
- Y. Ji, S. Gao, T. Huynh, C. Scheele, J. Triveri, J. Kruse, C. Bennett, and Y. Wen. Rethinking the regularity in mobility patterns of personal vehicle drivers: A multi-city comparison using a feature engineering approach. *Transactions in GIS*, 27(3):663–685, 2023. doi:[10.1111/tgis.13043](https://doi.org/10.1111/tgis.13043).
- R. Jiang, X. Song, Z. Fan, T. Xia, Q. Chen, S. Miyazawa, and R. Shibasaki. DeepUrbanMomentum: An Online Deep-Learning System for Short-Term Urban Mobility Prediction. *Proceedings of the AAAI Conference on Artificial Intelligence*, 32(1), 2018. doi:[10.1609/aaai.v32i1.11338](https://doi.org/10.1609/aaai.v32i1.11338).
- D. P. Kingma and J. Ba. Adam: A method for stochastic optimization. In *3rd International Conference on Learning Representations (ICLR '15)*, 2015.
- A. N. Koushik, M. Manoj, and N. Nezamuddin. Machine learning applications in activity-travel behaviour research: a review. *Transport Reviews*, 40(3):288–311, 2020. doi:[10.1080/01441647.2019.1704307](https://doi.org/10.1080/01441647.2019.1704307).
- V. Kulkarni and B. Garbinato. 20 years of mobility modeling & prediction: Trends, shortcomings & perspectives. In *Proceedings of the 27th International Conference on Advances in Geographic Information Systems (SIGSPATIAL '19)*, pages 492–495, 2019.
- X. Li, M. Feng, Y. Ran, Y. Su, F. Liu, C. Huang, H. Shen, Q. Xiao, J. Su, S. Yuan, and H. Guo. Big Data in Earth system science and progress towards a digital twin. *Nature Reviews Earth & Environment*, 4(5):319–332, 2023. doi:[10.1038/s43017-023-00409-w](https://doi.org/10.1038/s43017-023-00409-w).
- X. Lu, E. Wetter, N. Bharti, A. J. Tatem, and L. Bengtsson. Approaching the Limit of Predictability in Human Mobility. *Scientific Reports*, 3(1):2923, 2013. doi:[10.1038/srep02923](https://doi.org/10.1038/srep02923).
- M. Luca, G. Barlacchi, B. Lepri, and L. Pappalardo. A Survey on Deep Learning for Human Mobility. *ACM Computing Surveys*, 55:7:1–7:44, 2021. doi:[10.1145/3485125](https://doi.org/10.1145/3485125).
- Z. Ma and P. Zhang. Individual mobility prediction review: Data, problem, method and application. *Multimodal Transportation*, 1(1):100002, 2022. doi:[10.1016/j.multra.2022.100002](https://doi.org/10.1016/j.multra.2022.100002).
- E. L. Manibardo, I. Laña, and J. D. Ser. Deep Learning for Road Traffic Forecasting: Does it Make a Difference? *IEEE Transactions on Intelligent Transportation Systems*, 23(7):6164–6188, 2022. doi:[10.1109/tits.2021.3083957](https://doi.org/10.1109/tits.2021.3083957).
- C. Mao, A. Cha, A. Gupta, H. Wang, J. Yang, and C. Vondrick. Generative interventions for causal learning. In *Proceedings of the IEEE/CVF Conference on Computer Vision and Pattern Recognition (CVPR '21)*, pages 3947–3956, 2021.
- H. Martin, H. Becker, D. Bucher, D. Jonietz, M. Raubal, and K. W. Axhausen. Begleitstudie SBB Green Class - Abschlussbericht. *Arbeitsberichte Verkehrs- und Raumplanung*, 1439, 2019. doi:[10.3929/ethz-b-000353337](https://doi.org/10.3929/ethz-b-000353337).

- H. Martin, Y. Hong, N. Wiedemann, D. Bucher, and M. Raubal. Trackintel: An open-source python library for human mobility analysis. *Computers, Environment and Urban Systems*, 101:101938, 2023a. doi:[10.1016/j.compenvurbsys.2023.101938](https://doi.org/10.1016/j.compenvurbsys.2023.101938).
- H. Martin, N. Wiedemann, D. J. Reck, and M. Raubal. Graph-based mobility profiling. *Computers, Environment and Urban Systems*, 100:101910, 2023b. doi:[10.1016/j.compenvurbsys.2022.101910](https://doi.org/10.1016/j.compenvurbsys.2022.101910).
- N. Moshkov, M. Bornholdt, S. Benoit, M. Smith, C. McQuin, A. Goodman, R. A. Senft, Y. Han, M. Babadi, P. Horvath, B. A. Cimini, A. E. Carpenter, S. Singh, and J. C. Caicedo. Learning representations for image-based profiling of perturbations. *Nature Communications*, 15(1):1594, 2024. doi:[10.1038/s41467-024-45999-1](https://doi.org/10.1038/s41467-024-45999-1).
- L. Pappalardo, F. Simini, S. Rinzivillo, D. Pedreschi, F. Giannotti, and A.-L. Barabási. Returners and explorers dichotomy in human mobility. *Nature Communications*, 6(1):8166, 2015. doi:[10.1038/ncomms9166](https://doi.org/10.1038/ncomms9166).
- L. Pappalardo, E. Manley, V. Sekara, and L. Alessandretti. Future directions in human mobility science. *Nature Computational Science*, 3(7):588–600, 2023. doi:[10.1038/s43588-023-00469-4](https://doi.org/10.1038/s43588-023-00469-4).
- N. Pawlowski, D. Coelho de Castro, and B. Glocker. Deep structural causal models for tractable counterfactual inference. In *Proceedings of the 34th International Conference on Neural Information Processing Systems (NIPS '20)*, volume 33, pages 857–869, 2020.
- J. Pearl and D. Mackenzie. *The Book of Why: The New Science of Cause and Effect*. Basic Books, Inc., 1st edition, 2018. ISBN 978-0-465-09760-9.
- S. Rahimi, A. B. Moore, P. A. Whigham, and P. Dillingham. Counterfactual reasoning in space and time: Integrating graphical causal models in computational movement analysis. *Transactions in GIS*, 2023. doi:[10.1111/tgis.13100](https://doi.org/10.1111/tgis.13100).
- S. Ramezani, K. Hasanzadeh, T. Rinne, A. Kajosaari, and M. Kyttä. Residential relocation and travel behavior change: Investigating the effects of changes in the built environment, activity space dispersion, car and bike ownership, and travel attitudes. *Transportation Research Part A: Policy and Practice*, 147:28–48, 2021. doi:[10.1016/j.tra.2021.02.016](https://doi.org/10.1016/j.tra.2021.02.016).
- J. Runge, A. Gerhardus, G. Varando, V. Eyring, and G. Camps-Valls. Causal inference for time series. *Nature Reviews Earth & Environment*, 4(7):487–505, 2023. doi:[10.1038/s43017-023-00431-y](https://doi.org/10.1038/s43017-023-00431-y).
- C. Santana, F. Botta, H. Barbosa, F. Privitera, R. Menezes, and R. Di Clemente. COVID-19 is linked to changes in the time–space dimension of human mobility. *Nature Human Behaviour*, pages 1–11, 2023. doi:[10.1038/s41562-023-01660-3](https://doi.org/10.1038/s41562-023-01660-3).
- C. M. Schneider, V. Belik, T. Couronné, Z. Smoreda, and M. C. González. Unravelling daily human mobility motifs. *Journal of The Royal Society Interface*, 10(84):20130246, 2013. doi:[10.1098/rsif.2013.0246](https://doi.org/10.1098/rsif.2013.0246).
- B. Schölkopf, F. Locatello, S. Bauer, N. R. Ke, N. Kalchbrenner, A. Goyal, and Y. Bengio. Toward Causal Representation Learning. *Proceedings of the IEEE*, 109(5):612–634, 2021. doi:[10.1109/JPROC.2021.3058954](https://doi.org/10.1109/JPROC.2021.3058954).
- S. Schönfelder and K. W. Axhausen. *Urban rhythms and travel behaviour: spatial and temporal phenomena of daily travel*. Routledge, 2016.
- R. Silva. Observational-interventional priors for dose-response learning. In *Proceedings of the 30th International Conference on Neural Information Processing Systems (NIPS '16)*, volume 29, pages 1569–1577, 2016.
- A. Solomon, A. Livne, G. Katz, B. Shapira, and L. Rokach. Analyzing movement predictability using human attributes and behavioral patterns. *Computers, Environment and Urban Systems*, 87:101596, 2021. doi:[10.1016/j.compenvurbsys.2021.101596](https://doi.org/10.1016/j.compenvurbsys.2021.101596).
- C. Song, T. Koren, P. Wang, and A.-L. Barabási. Modelling the scaling properties of human mobility. *Nature Physics*, 6(10):818–823, 2010a. doi:[10.1038/nphys1760](https://doi.org/10.1038/nphys1760).
- C. Song, Z. Qu, N. Blumm, and A.-L. Barabasi. Limits of Predictability in Human Mobility. *Science*, 327(5968):1018–1021, 2010b. doi:[10.1126/science.1177170](https://doi.org/10.1126/science.1177170).

- J. Sun and J. Kim. Joint prediction of next location and travel time from urban vehicle trajectories using long short-term memory neural networks. *Transportation Research Part C: Emerging Technologies*, 128:103114, 2021. doi:[10.1016/j.trc.2021.103114](https://doi.org/10.1016/j.trc.2021.103114).
- Y. O. Susilo and K. W. Axhausen. Repetitions in individual daily activity-travel-location patterns: a study using the Herfindahl-Hirschman Index. *Transportation*, 41(5):995–1011, 2014. doi:[10.1007/s11116-014-9519-4](https://doi.org/10.1007/s11116-014-9519-4).
- Y. Tang, N. Cheng, W. Wu, M. Wang, Y. Dai, and X. Shen. Delay-Minimization Routing for Heterogeneous VANETs With Machine Learning Based Mobility Prediction. *IEEE Transactions on Vehicular Technology*, 68(4):3967–3979, 2019. doi:[10.1109/TVT.2019.2899627](https://doi.org/10.1109/TVT.2019.2899627).
- D. d. C. Teixeira, A. C. Viana, M. S. Alvim, and J. M. Almeida. Deciphering Predictability Limits in Human Mobility. In *Proceedings of the 27th ACM SIGSPATIAL International Conference on Advances in Geographic Information Systems (SIGSPATIAL '19)*, pages 52–61, 2019. doi:[10.1145/3347146.3359093](https://doi.org/10.1145/3347146.3359093).
- D. d. C. Teixeira, J. M. Almeida, and A. C. Viana. On estimating the predictability of human mobility: the role of routine. *EPJ Data Science*, 10(1):1–30, 2021. doi:[10.1140/epjds/s13688-021-00304-8](https://doi.org/10.1140/epjds/s13688-021-00304-8).
- W. van Amsterdam, J. Verhoeff, P. de Jong, T. Leiner, and M. Eijkemans. Eliminating biasing signals in lung cancer images for prognosis predictions with deep learning. *npj Digital Medicine*, 2(1):1–6, 2019.
- A. Vaswani, N. Shazeer, N. Parmar, J. Uszkoreit, L. Jones, A. N. Gomez, L. Kaiser, and I. Polosukhin. Attention is All you Need. In *Proceedings of the 31st International Conference on Neural Information Processing Systems (NIPS '17)*, volume 30, pages 5998–6008, 2017.
- N. Wiedemann, Y. Hong, and M. Raubal. Predicting visit frequencies to new places. In *12th International Conference on Geographic Information Science (GIScience '23)*, volume 277, pages 84:1–84:6, 2023a. doi:[10.4230/LIPICs.GIScience.2023.84](https://doi.org/10.4230/LIPICs.GIScience.2023.84).
- N. Wiedemann, H. Martin, E. Suel, Y. Hong, and Y. Xin. Influence of tracking duration on the privacy of individual mobility graphs. *Journal of Location Based Services*, 0(0):1–19, 2023b. doi:[10.1080/17489725.2023.2239190](https://doi.org/10.1080/17489725.2023.2239190).
- Y. Xin, N. Tagasovska, F. Perez-Cruz, and M. Raubal. Vision paper: causal inference for interpretable and robust machine learning in mobility analysis. In *Proceedings of the 30th International Conference on Advances in Geographic Information Systems (SIGSPATIAL '22)*, pages 1–4, 2022. doi:[10.1145/3557915.3561473](https://doi.org/10.1145/3557915.3561473).
- Y. Xu, A. Belyi, I. Bojic, and C. Ratti. Human mobility and socioeconomic status: Analysis of Singapore and Boston. *Computers, Environment and Urban Systems*, 72:51–67, 2018a. doi:[10.1016/j.compenvurbsys.2018.04.001](https://doi.org/10.1016/j.compenvurbsys.2018.04.001).
- Y. Xu, S. Çolak, E. C. Kara, S. J. Moura, and M. C. González. Planning for electric vehicle needs by coupling charging profiles with urban mobility. *Nature Energy*, 3(6):484–493, 2018b. doi:[10.1038/s41560-018-0136-x](https://doi.org/10.1038/s41560-018-0136-x).
- Y. Xu, D. Zou, S. Park, Q. Li, S. Zhou, and X. Li. Understanding the movement predictability of international travelers using a nationwide mobile phone dataset collected in South Korea. *Computers, Environment and Urban Systems*, 92:101753, 2022. doi:[10.1016/j.compenvurbsys.2021.101753](https://doi.org/10.1016/j.compenvurbsys.2021.101753).
- X.-Y. Yan, W.-X. Wang, Z.-Y. Gao, and Y.-C. Lai. Universal model of individual and population mobility on diverse spatial scales. *Nature Communications*, 8(1):1639, 2017. doi:[10.1038/s41467-017-01892-8](https://doi.org/10.1038/s41467-017-01892-8).
- X. Yin, G. Wu, J. Wei, Y. Shen, H. Qi, and B. Yin. Deep Learning on Traffic Prediction: Methods, Analysis, and Future Directions. *IEEE Transactions on Intelligent Transportation Systems*, 23(6):4927–4943, 2022. doi:[10.1109/tits.2021.3054840](https://doi.org/10.1109/tits.2021.3054840).
- C. Zhao, A. Zeng, and C. H. Yeung. Characteristics of human mobility patterns revealed by high-frequency cell-phone position data. *EPJ Data Science*, 10(1), 2021. doi:[10.1140/epjds/s13688-021-00261-2](https://doi.org/10.1140/epjds/s13688-021-00261-2).
- K. Zhao, M. Musolesi, P. Hui, W. Rao, and S. Tarkoma. Explaining the power-law distribution of human mobility through transportation modality decomposition. *Scientific Reports*, 5(1):9136, 2015. doi:[10.1038/srep09136](https://doi.org/10.1038/srep09136).

Z. Zhao, H. N. Koutsopoulos, and J. Zhao. Individual mobility prediction using transit smart card data. *Transportation Research Part C: Emerging Technologies*, 89:19–34, 2018. doi:[10.1016/j.trc.2018.01.022](https://doi.org/10.1016/j.trc.2018.01.022).